https://doi.org/10.5194/acp-2020-1113
Preprint. Discussion started: 14 January 2021

Atmospheric Chemistry and Physics
Discussions

Estimating Radiative Forcing Efficiency of Dust Aerosol Based on Direct Satellite Observations: Case Studies over the Sahara Desert and Taklimakan Desert

Lin Tian[1,2,3], Lin Chen[3], Peng Zhang[3], Lei Bi[4]

[1] Nanjing University of Information Science & Technology, Nanjing, China.
[2] Chinese Academy of Meteorological Sciences, Beijing, China.
[3] National Satellite Meteorological Center, China Meteorological Administration, Beijing, China.
[4] Department of Atmospheric Sciences, School of Earth Sciences, Zhejiang University, Hangzhou, China.

Correspondence to: Peng Zhang (zhangp@cma.gov.cn) & Lin Chen (chenlin@cma.gov.cn)

Abstract. The direct radiative forcing efficiency of the dust aerosol ($DRFE_{dust}$) is an important indicator to measure the climate effect of the dust. The $DRFE_{dust}$ is determined by the microphysical properties of the dust, which vary with the dust source regions. However, there are only sparse in-situ measurements of them, such as the distribution of the dust aerosol particle size and the complex refractive index in the main dust source regions. Furthermore, recent studies have shown that the non-spherical effect of the dust particle is not negligible. The $DRFE_{dust}$ is often evaluated by estimating given microphysical properties of the dust aerosols in the radiative transfer model (RTM). However, considerable uncertainties exist due to the complex and variable dust properties, including the complex refractive index and the shape of the dust. The $DRFE_{dust}$ over the Taklimakan Desert and the Sahara Desert is derived from the satellite observations in this paper. The advantage of the proposed satellite-based method is that there is no need to consider the microphysical properties of the dust aerosols in estimating the $DRFE_{dust}$. For comparison, the observed $DRFE_{dust}$ is compared with that simulated by the RTM. The differences in the dust microphysical properties in these two regions and their impacts on $DRFE_{dust}$ are analyzed.

The $DRFE_{dust}$ derived from the satellite observation is -39.6 ± 10.0 $Wm^{-2}\tau^{-1}$ in March 2019 over Tamanrasset and -48.6 ± 13.7 $Wm^{-2}\tau^{-1}$ in April 2019 over Kashi. According to the analyses of their microphysical properties and optical properties, the dust aerosols from the Taklimakan desert (Kashi) scatter strongly. The RTM simulated results (-41.5 to -47.4 $Wm^{-2}\tau^{-1}$ in the Taklimakan Desert and -32.2 to -44.3 $Wm^{-2}\tau^{-1}$ in the Sahara Desert) are in good agreement with the results estimated by satellite observations. According to previous studies, the results in this paper are proved to be

https://doi.org/10.5194/acp-2020-1113
Preprint. Discussion started: 14 January 2021

Atmospheric Chemistry and Physics Discussions

reasonable and reliable. The results also show that the microphysical properties of the dust can significantly influence the DRFE$_{dust}$. The satellite-derived results can represent the influence of the dust microphysical properties on the DRFE$_{dust}$, which can also validate the direct radiative effect of the dust aerosol and the DRFE$_{dust}$ derived from numerical model more directly.

1 Introduction

Dust aerosols are considered to be one of the major components of the tropospheric aerosols (Huneeus et al., 2012;Textor et al., 2007). The dust aerosols affect the radiation balance of the earth-atmosphere system by scattering and absorbing solar radiation directly (Miller et al., 2014;Satheesh, 2002). Estimating the direct radiation effect of the dust aerosol (DRE$_{dust}$) is crucial for estimating climate forcing. The scattering of the dust influences the radiation in the shortwave (SW) spectrum at the top of atmosphere (TOA), which causes stronger SW DRE$_{dust}$ over dust source regions (Slingo et al., 2006). Therefore, the evaluation of SW DRE$_{dust}$ is important for climate modeling.

The variabilities of the mineral dust composition from soils in different source regions cause the differences in dust microphysical properties (e.g., refractive index, size, and particle shapes). Anderson et al. (2005) defined the Direct Radiative Forcing Efficiency of the dust aerosol (DRFE$_{dust}$) to quantify the dust radiative effect (Anderson et al., 2005). The DRFE$_{dust}$ represents the DRE$_{dust}$ of a certain aerosol optical depth (AOD) at per unit area, which means the efficiency of the dust aerosol that affects the net radiative flux of solar radiation. The DRFE$_{dust}$ is largely determined by the optical properties of the dust aerosols (Shi et al., 2005), which are strictly controlled by the microphysical properties of the particles (Di Biagio et al., 2014b;Di Biagio et al., 2017;Di Biagio et al., 2014a;Zhang et al., 2006). Therefore, the DRFE$_{dust}$ is different concerning the dust aerosols from different source regions (Tanré et al., 2001;Che et al., 2012). Without considering the influence of the aerosol loading on the DRE$_{dust}$, the DRFE$_{dust}$ has unique advantages in evaluating the differences of dust microphysical properties and their impacts on the DRE$_{dust}$ from different dust source regions (García et al., 2008).

The DRFE$_{dust}$ is often estimated by the General Circulation Model (GCM) and the Radiative Transfer Model (RTM). Many studies have simulated the SW DRFE$_{dust}$ in different regions (Valenzuela et al., 2012;Che et al., 2009;Bi et al., 2014). However, there are sparse in-situ measurements of the dust microphysical properties in the main source regions. The large spatial

https://doi.org/10.5194/acp-2020-1113
Preprint. Discussion started: 14 January 2021

variability of aerosols and the lack of an adequate database on their properties makes DRE_{dust} and $DRFE_{dust}$ much difficult to estimated (Satheesh and Srinivasan, 2006). To date, climate models generally use temporal and spatial constant values to represent the dust microphysical properties (Di Biagio et al., 2017;Di Biagio et al., 2014a;Bi et al., 2020). This may cause uncertainties in calculating the dust radiative effect. Moreover, the shape of the dust particle in the model needs to be assumed. Therefore, there are large uncertainties in estimating the $DRFE_{dust}$ with few measurements of the dust microphysical properties from different source regions (Bi et al., 2020;Colarco et al., 2014;Zhao et al., 2013).

Satellite observations can be used in estimating the $DRFE_{dust}$ because satellites can directly observe the radiation budget of the earth in the TOA (Wielicki et al., 1998;Satheesh and Ramanathan, 2000), and the remote-sensing technique for the AOD has been developed (Remer et al., 2005;Hsu et al., 2004). In the previous study, we developed a satellite-based method to estimate the $DRFE_{dust}$ over land without any assumptions of the microphysical properties of dust aerosols (Tian et al., 2019). In previous researches, performances of the models in simulating the dust radiative effect have been indirectly validated by comparing the observations of the AOD, the single scattering albedo (SSA), the distribution of the particle size, and the extinction profile of the aerosols with the simulated ones (Zhao et al. 2010; Chen et al. 2014). Therefore, the satellite-based method provides a direct way to validate the DRE_{dust} and the $DRFE_{dust}$.

The Taklimakan Desert and the Sahara Desert are the main dust source regions, which influence many areas (Li et al., 2020;Mikami et al., 2006;Mbourou et al., 1997;Huang et al., 2014). Thus, the assessment of the SW $DRFE_{dust}$ and microphysical properties of the dust over these regions is important for evaluating regional and global climate changes.

In this paper, the $DRFE_{dust}$ in dust storms over the Taklimakan Desert and the Sahara Desert is evaluated based on satellite observations and the RTM, separately. With the comparison of the dust microphysical properties and the $DRFE_{dust}$ in these two regions, the differences of the dust microphysical properties are analyzed. Meanwhile, the influences of the dust microphysical properties on the $DRFE_{dust}$ are investigated in this paper. The need for accurate information on the dust microphysical properties and dust sources for simulating the $DRFE_{dust}$ is emphasized, and the advantage of the satellite-based method in estimating the $DRFE_{dust}$ is revealed.

https://doi.org/10.5194/acp-2020-1113
Preprint. Discussion started: 14 January 2021

2 Methodology and data

In the previous study (Tian et al., 2019), the equi-albedo method has been proposed to estimate the DRE_{dust} and the $DRFE_{dust}$ over land based on satellite measurements directly. This method bases on the assumption that the SW radiative fluxes at the TOA of the clear sky (F_{clr}) are equal over the regions with similar land surface albedo (LSA) and solar zenith angle (SZA). Following this method, we estimated the $DRFE_{dust}$ based on the AOD and the SW radiative flux product from the same satellite platform.

Moreover, the $DRFE_{dust}$ in the RTM with dust aerosol microphysical properties is also evaluated. Based on the comparison between the $DRFE_{dust}$ results from the two methods, the differences in the dust microphysical properties over the Taklimakan Desert and the Sahara Desert are analyzed, and the differences in the $DRFE_{dust}$ are also discussed. The processing steps are shown in Fig. 1.

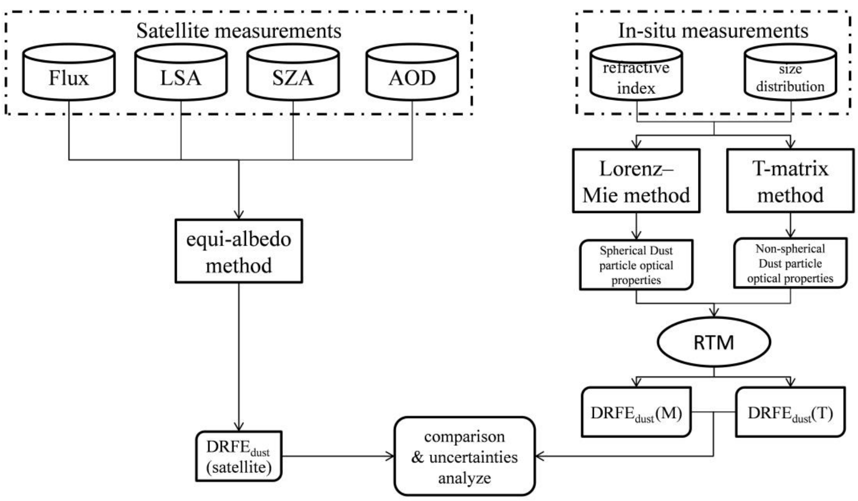

Flux: Radiative Flux observed by CERES;
LSA: Land Surface Albedo;
SZA: Solar zenith Angle;
AOD: Aerosol Optical Depth;
$DRFE_{dust}$(satellite): $DRFE_{dust}$ estimated from satellite measurements
$DRFE_{dust}$(M): $DRFE_{dust}$ simulated from Lorenz–Mie method and RTM;
$DRFE_{dust}$(T): $DRFE_{dust}$ simulated from T-matrix method and RTM;

Figure 1: Processing flow chart of this paper.

https://doi.org/10.5194/acp-2020-1113
Preprint. Discussion started: 14 January 2021

Atmospheric Chemistry and Physics Discussions

2.1 Methodology

2.1.1 The equi-albedo method

Previous studies have shown that F_{clr} is significantly influenced by the LSA and the SZA at the TOA (Di Biagio et al., 2012;Tegen et al., 2010). It is hard to assess the SW DRE_{dust} and the $DRFE_{dust}$ over land derived from satellite observations due to the large dynamic range of the LSA (Satheesh, 2002). In the previous study (Tian et al., 2019), we proposed an equi-albedo method to minimize the influence of the inhomogeneous LSA and SZA and directly derived the DRE_{dust} and the $DRFE_{dust}$ over land from satellite observations based on the assumption that the F_{clr} is equal over the regions with similar LSA and SZA.

DRE_{dust} was defined as the radiative fluxes difference between clear (F_{clr}) and dust loading (F_{dust}) conditions (Garrett and Zhao, 2006;Christopher et al., 2000;Ramanathan et al., 1989).

$$DRE_{dust} = F_{clr} - F_{dust} \quad (1).$$

F_{dust} is the shortwave radiative flux at TOA in the cloud-free and dust aerosol loading condition which is obtained directly from CERES data, and F_{clr} is the shortwave flux over the same region without aerosol. F_{clr} cannot be observed directly, and the estimating of F_{clr} must be on the basis of some realistic assumptions.

The equi-albedo method bases on the assumption that the SW radiative fluxes at the TOA of the clear sky (F_{clr}) are equal over the regions with similar land surface albedo (LSA) and solar zenith angle (SZA). Based on the assumption, the F_{clr} were estimated, then DRE_{dust} can be derived following Eq. (1). According to the definition of $DRFE_{dust}$, it represents the net flux of solar radiation perturbed by per unit dust AOD. Therefore, $DRFE_{dust}$ can be expressed as:

$$DRFE_{dust} = DRE_{dust}/\tau_{dust} \quad (2)$$

where τ_{dust} is the AOD of dust aerosols, and τ_{dust} comes from the MODIS aerosol product. Thus, $DRFE_{dust}$ was estimated based on the AOD and the SW radiative flux product from the same satellite platform.

In the previous study (Tian et al., 2019), we have estimated the DRE_{dust} and the $DRFE_{dust}$ of two dust storms in the Taklimakan Desert. The results were compared with the DRE_{dust} and the $DRFE_{dust}$ simulated by the RTM. The results indicated that the method is effective in estimating the SW $DRFE_{dust}$ over land. The microphysical properties of dust aerosols significantly influence on the DRE_{dust} and the $DRFE_{dust}$ (Che et al., 2012;Li et al., 2018). The different microphysical properties of dust aerosols in

https://doi.org/10.5194/acp-2020-1113
Preprint. Discussion started: 14 January 2021

Atmospheric Chemistry and Physics Discussions

various dust source regions cause uncertainties in estimating the SW DRE_{dust} and $DRFE_{dust}$. Thus, the equi-albedo method is used to estimate the SW $DRFE_{dust}$ directly using satellite observations in this study. Based on the comparison of the $DRFE_{dust}$ in the Taklimakan Desert and the Sahara Desert, the differences of dust microphysical properties in these two regions are analyzed and the influences of the dust microphysical properties on estimating the $DRFE_{dust}$ are tested.

2.1.2 Calculating method of dust optical properties

Dust aerosols are often assumed as spherical particles in the GCM and the RTM (Wang et al., 2013;Gao and Anderson, 2001). The Lorenz-Mie theory is used to calculate the optical properties of the dust particles (Gouesbet and Gréhan, 2011). However, observations and researches have shown that most dust aerosols are non-spherical in nature (Nakajima et al., 1989;Okada et al., 2001). Previous researches also suggested that assuming particles as spherical or non-spherical has significant impacts on calculating the dust optical properties (Kalashnikova and Sokolik, 2004;Borghese et al., 2007). Therefore, the optical properties of dust aerosols are calculated using both the spherical and the ellipsoidal methods for comparison to analyze the uncertainties caused by the assumption of dust shapes in estimating the $DRFE_{dust}$ in this study.

To make it more accurate, the light scattering properties of spherical particles are generally calculated based on the Mie and Lorenz theory (Mishchenko and Travis, 2008). Among several methods for computing optical properties of non-spherical particles, the T-matrix method has been extensively developed to many versions for various applications (Chylek et al., 1977;Mishchenko et al., 1996). These versions of the available T-matrix code are accessed from the National Aeronautics and Space Administration (NASA) Goddard Institute for Space Studies (GISS) group (Mishchenko and Travis, 1998). Mie scattering method can be regarded as a special case of the T-matrix method. In this study, the NASA-GISS code is used to calculate the optical properties of the spherical particles and the ellipsoidal particles. The particle aspect ratio is set to 0.8.

2.1.3 RTM

Santa Barbara Disort Atmospheric Radiative Transfer (SBDART) is an RTM that calculates the plane-parallel radiative transfer of the earth-atmosphere system (Ricchiazzi et al., 1998). The broadband radiative flux at the TOA and the surface in clear-sky and dusty conditions can be obtained. It is

https://doi.org/10.5194/acp-2020-1113
Preprint. Discussion started: 14 January 2021

Atmospheric Chemistry and Physics Discussions

conducive to analyzing the radiative transfer theory in satellite remote sensing and atmospheric energy budget studies. Furthermore, the model can flexibly set up aerosol properties, which is well suited to calculate the radiative effect of different types of aerosols. The SBDART model has been widely used in estimating the $DRFE_{dust}$ due to its design (Chen et al., 2011;Li et al., 2020;Iftikhar et al., 2018).

In this paper, the dust aerosol optical properties (the SSA and the ASYmmetry parameter, abbreviated as ASY) are calculated using spherical and non-spherical methods. The Aerosol Robotic Network (AERONET) inversion products, the LSA from Moderate Resolution Imaging Spectroradiometer (MODIS) surface albedo product, and the default atmospheric profile of SBDART (MID-LATITUDE WINTER) are used as the input parameters for the SBDART model in simulating the $DRFE_{dust}$. Therefore, the DRE_{dust} changing with the AOD due to both dust aerosol microphysical properties (including the complex refractive index and the distribution of the size) and optical properties (including the SSA and the ASY) are simulated by the SBDART model. The impacts of the microphysical properties and the optical properties of the dust aerosol on the DRE_{dust} are analyzed in this study.

2.2 Data

This paper aims to analyze the differences in dust microphysical properties and the $DRFE_{dust}$ over the Taklimakan Desert and the Sahara Desert to confirm the influences of dust aerosol microphysical properties on simulating the $DRFE_{dust}$. Also, the advantages of the satellite-based method in estimating the $DRFE_{dust}$ are analyzed. Therefore, the $DRFE_{dust}$ over the Taklimakan Desert and the Sahara Desert is estimated by using both satellite observations and dust microphysical properties.

https://doi.org/10.5194/acp-2020-1113
Preprint. Discussion started: 14 January 2021

Atmospheric Chemistry and Physics Discussions

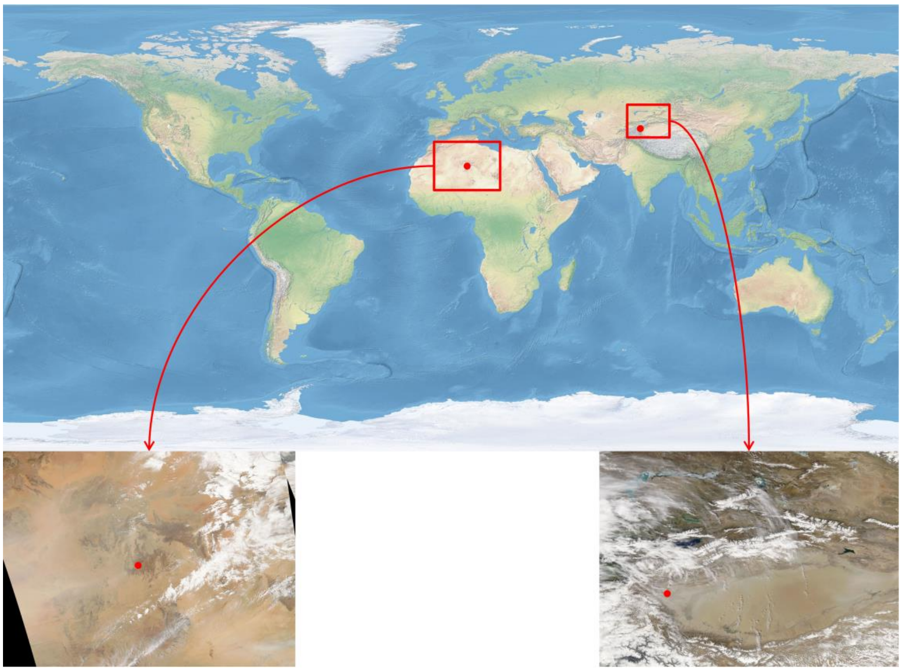

Figure 2: The research regions and dust storms viewed by MODIS Aqua on 11 March and 9 April 2019.

Fig. 2 shows the research regions (the red square areas) and the locations of in-situ sites (Tamanrasset site and Kashi site, the red dots in the map and satellite images). Tamanrasset (22.79˚N, 5.53˚E, 1377 m above the mean sea level) locates in southern Algeria, which is free from the influence of industrial activities. Thus, the aerosols measured in Tamanrasset can represent the pure dust aerosols from the Sahara Desert (Guirado-Fuentes et al., 2014). Kashi (39.5˚N, 75.9˚E, 1320 m above the mean sea level) locates in the vicinity of the Taklimakan Desert. Kashi represents a place affected by dust aerosols transported from the Taklimakan Desert (Li et al., 2020). Thus, dust aerosols observed in Tamanrasset and Kashi sites are typical samples of the dust aerosols from these two deserts. Moreover, Tamanrasset and Kashi sites are similar in land surface type, altitude, and climate. As the LSA and the SZA have a great impact on the SW radiative effect, the regions with similar LSA and SZA are chosen to avoid the influence of different LSA and SZA on evaluating the differences of dust microphysical properties and dust radiative effect from different dust source regions.

A dust storm occurred on 11 March 2019 in Tamanrasset. In Kashi, a dust storm occurred on 9 April 2019. These dust storms are shown visually by Aqua MODIS (Fig. 2). Fig. 3 shows the LSA and the SZA observed by the AQUA satellite on 11 March 2019 in the Sahara Desert and on 25 April 2019

https://doi.org/10.5194/acp-2020-1113
Preprint. Discussion started: 14 January 2021

Atmospheric Chemistry and Physics
Discussions

in Taklimakan Desert. In Fig. 3, the LSA and the SZA are similar in Tamanrasset and Kashi when the satellite passes through. The data around Tamanrasset and Kashi in March and April are suitable for analyzing the differences of dust microphysical properties and their influences on the $DRFE_{dust}$.

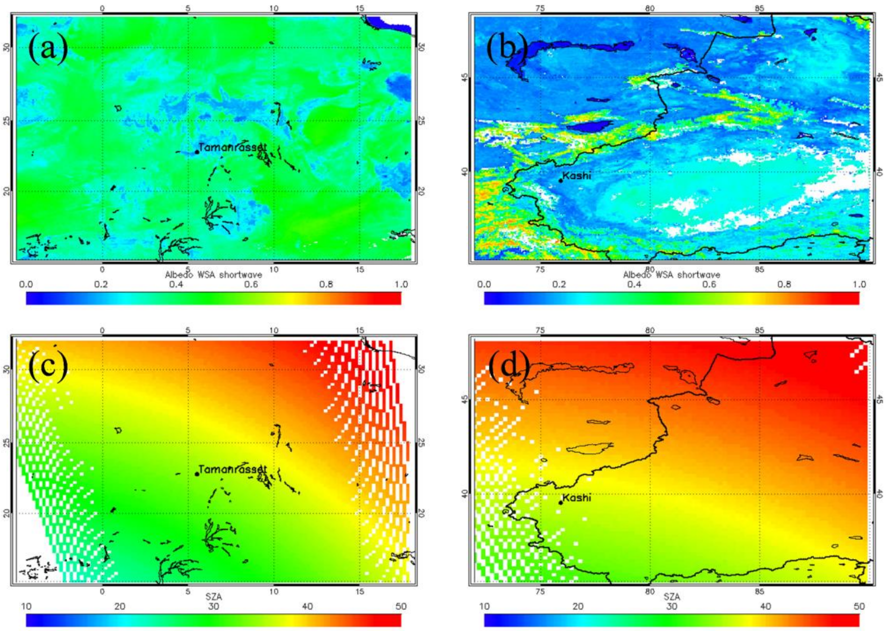

Figure 3: (a) MODIS SW LSA and (c) SZA on 11 March 2019 over Tamanrasset; (b) MODIS SW LSA and (d) SZA on 24 April 2010 over Kashi.

The satellite-observed and dust microphysical properties data of the dust storms in March and April 2019 in Tamanrasset and Kashi are collected to analyze the dust microphysical properties and estimate the $DRFE_{dust}$ in the Taklimakan Desert and the Sahara Desert. Fig. 4 shows the satellite images of these dust storms, which can be seen from the satellite images in cloud-free conditions over Tamanrasset (left column of Fig. 4, Fig. 4(a), Fig. 4(c), Fig. 4(e)) and Kashi (right column of Fig. 4, Fig. 4(b), Fig. 4(d), Fig. 4(f)). Both the satellite data and synergy dust microphysical properties data are collected around Tamanrasset and Kashi sites for analyzing the differences in dust microphysical properties and estimating the $DRFE_{dust}$.

https://doi.org/10.5194/acp-2020-1113
Preprint. Discussion started: 14 January 2021

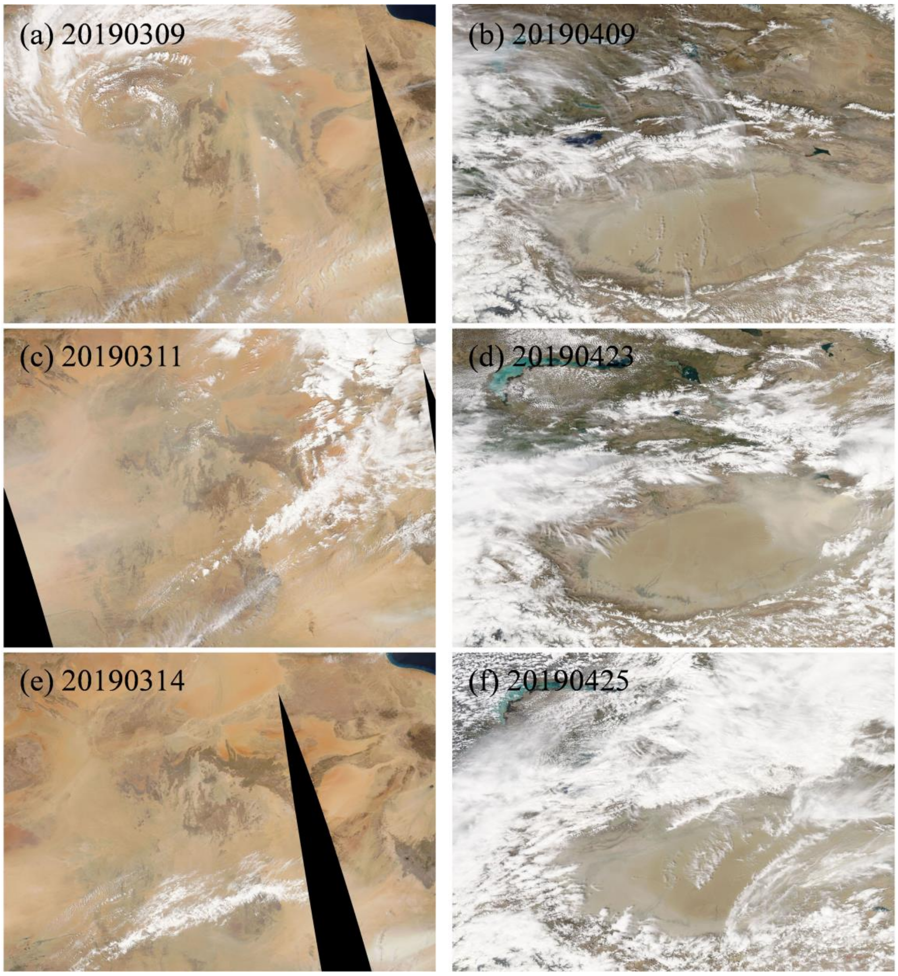

Figure 4: Dust storms viewed by AQUA/MODIS over target areas (Tamanrasset and Kashi).

2.2.1 Satellite data

MODIS and CERES (Clouds and the Earth's Radiant Energy System) are the key instruments of the AQUA and the TERRA satellite and are important in NASA's Earth Observing System (EOS). The AOD products from MODIS and the radiative flux products at the TOA from CERES can be synergistically used to estimate the $DRFE_{dust}$ directly.

Several algorithms have been developed for MODIS AOD remote-sensing products after MODIS instruments were launched (Remer et al., 2005). Of these algorithms, the Deep Blue algorithm (Hsu et al., 2004) solved the problems in aerosol retrieval by satellite remote-sensing for high reflectance land surface types (such as arid, semi-arid, and desert areas), and retried the AOD over high reflectance land

https://doi.org/10.5194/acp-2020-1113
Preprint. Discussion started: 14 January 2021

surface types. In this paper, the deep blue AOD (0.55μm) data are used to discriminate the dust storm regions. The LSA is also needed both in the satellite-based equi-albedo method and the RTM. The MODIS Collection6 albedo product dataset (MCD43C3) (Schaaf et al., 2011;Schaaf et al., 2002;Schaaf et al., 2008) provides high-quality land surface reflectance and albedo data over various types of land surfaces by using anisotropy retrievals algorithm (Jin et al., 2003;Liang et al., 2002;Liu et al., 2009;Román et al., 2010). The MCD43C3 product dataset is available from the Land Processes Distributed Active Archive Center (LP DAAC) of NASA. The white-sky albedo from the MCD43C3 product is used to get the SW broadband LSA.

CERES single scanner footprint (SSF) level 2 dataset can provide the radiative flux at the TOA in three broadband channels. Here the instantaneous SW channel (0.3–5.0 μm) radiative flux at the TOA from CERES SSF level 2 dataset is used. MODIS and CERES are onboard in the same satellite platform (AQUA). The radiative flux derived from CERES is co-located with the MODIS scene. The DRE_{dust} and the $DRFE_{dust}$ at the TOA are estimated by synergistically using MODIS and CERES products.

2.2.2 Dust microphysical properties data

The Aerosol Robotic Network (AERONET) is the largest ground-based network for measuring aerosols with more than 400 sites installed.

The AERONET provides microphysical properties and optical properties of the aerosols at four wavelengths (440, 675, 870, and 1020 nm). The AOD product is directly measured by the sun photometer. The inversion algorithm retrieves the physical properties of aerosols such as volume size distributions and the complex refractive index, and optical properties such as the SSA and the ASY (Dubovik and King, 2000;Dubovik et al., 2006).

https://doi.org/10.5194/acp-2020-1113
Preprint. Discussion started: 14 January 2021

Atmospheric Chemistry and Physics
Open Access
EGU
Discussions

3 DRFE$_{dust}$ estimated based on satellite observations

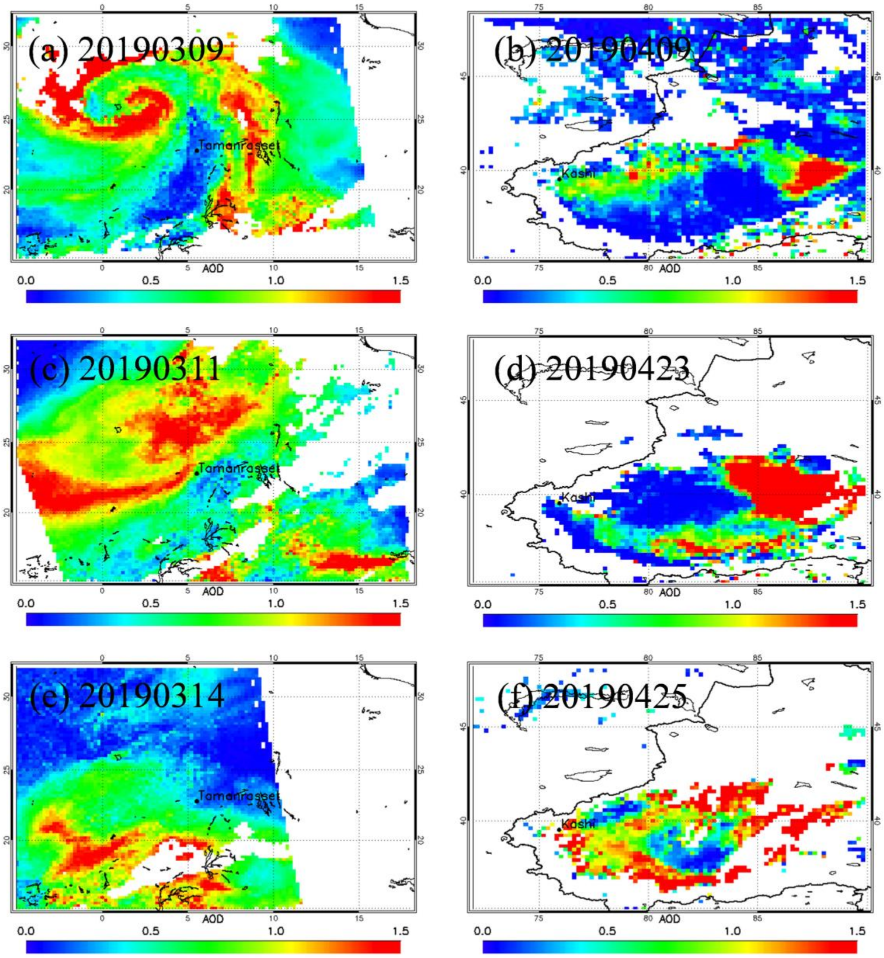

Figure 5: AOD at 0.55 μm (τ_{550}) of the dust storm in March 2019 over Tamanrasset and that in April 2019 over Kashi.

MODIS L2 deep blue AOD product of the dust storm in March 2019 over Tamanrasset and that in April 2019 over Kashi are shown in Fig. 5. The missing data are shown in white; the high dust loading regions are shown in red; the low dust loading regions are shown in blue. Fig. 5 shows that there are heavy dust storms over Tamanrasset and Kashi with AOD great than 1.0 detected by MODIS.

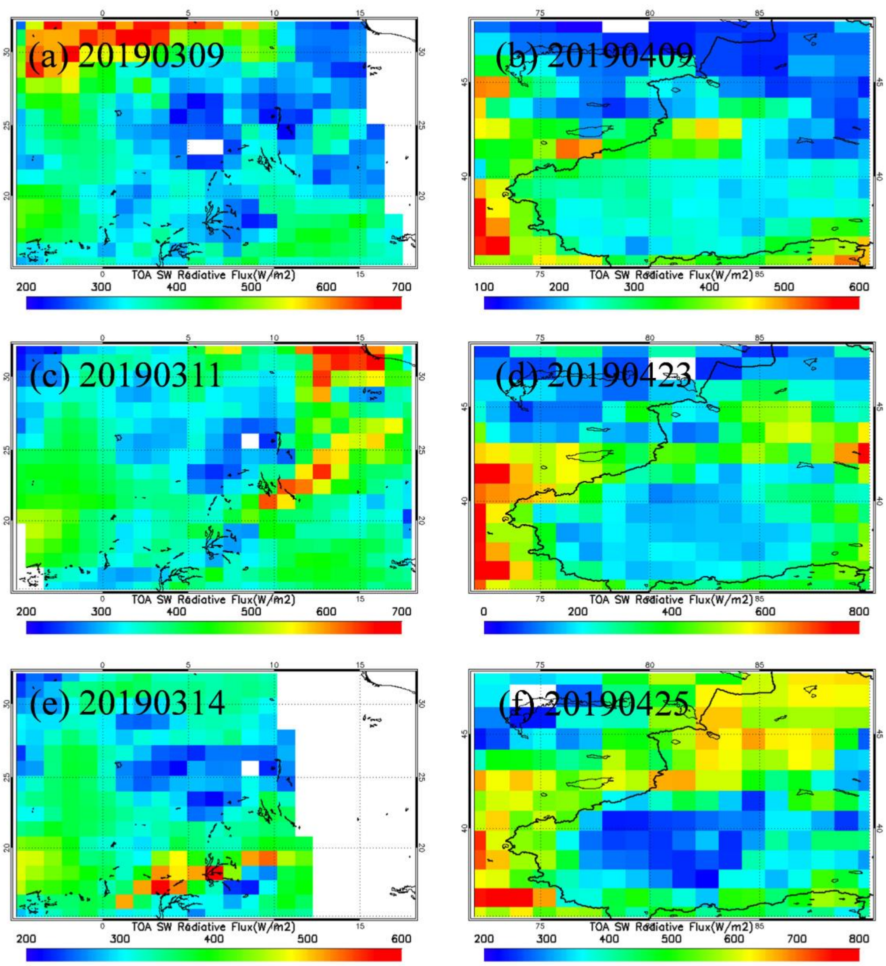

Figure 6: TOA SW radiative flux in March 2019 over Tamanrasset and that in April 2019 over Kashi.

Fig. 6 shows the TOA SW radiative flux measured by CERES in March 2019 over Tamanrasset and that in April 2019 over Kashi during the dust storms. The TOA SW radiative flux distribution shows the highest value over cloud conditions. The values in dust storm regions are higher than those in clear-sky regions. It is due to the fact that the SW albedo of the aerosols in the cloud and the dust is higher than those on the land surface. Thus, dust aerosols have a negative radiative effect in the SW spectrum. Following the equi-albedo method (Tian et al., 2019), the DRE_{dust} is estimated based on the measurements from MODIS and CERES both aboard on the AQUA satellite.

As Fig. 4, Fig. 5 and Fig. 6 shown, the spatial resolution of TOA flux from CERES/SSF product is 1 °×1 °grid, and LSA, SZA, AOD data from satellite have the different spatial resolution. In order to

https://doi.org/10.5194/acp-2020-1113
Preprint. Discussion started: 14 January 2021

match up LSA, SZA and AOD data with CERES TOA SW fluxes, we have resampled LSA, SZA and AOD data into CERES SSF product horizontal spatial resolution. Then the F_{clr} and DRE_{dust} over Tamanrasset and Kashi can be estimated following equi-albedo method.

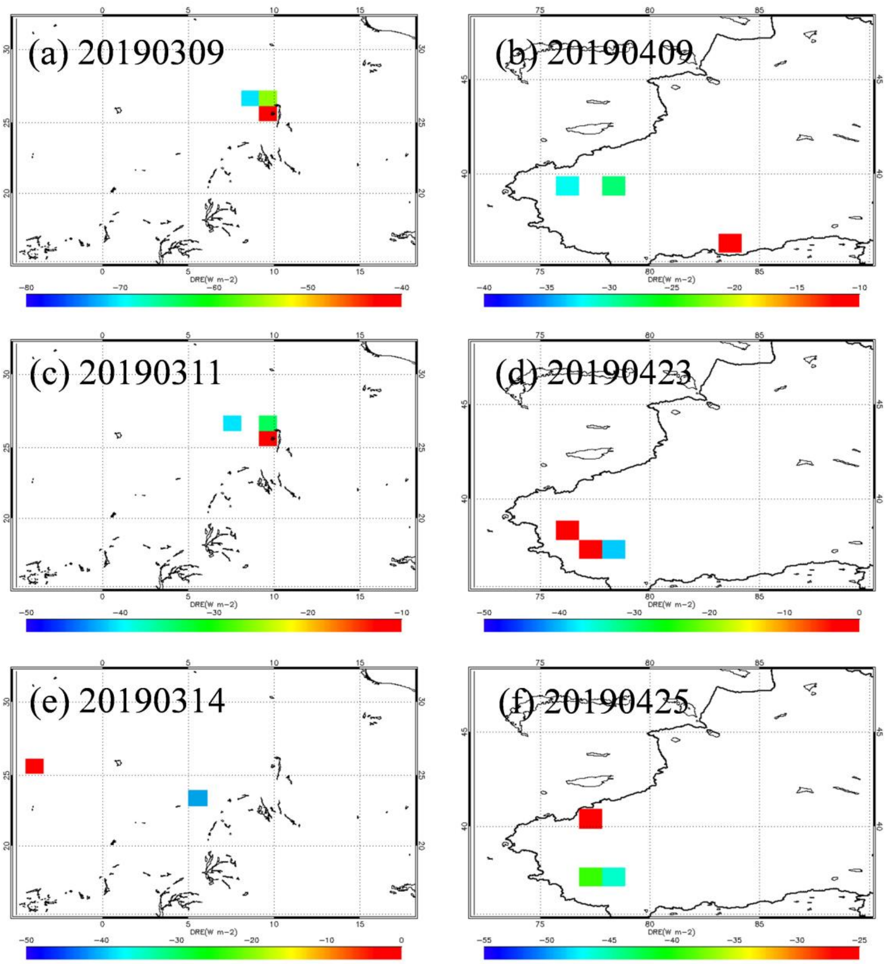

Figure 7: DRE_{dust} on March 2019 over Tamanrasset and on April 2019 over Kashi.

Fig. 7 shows the distribution maps of the DRE_{dust}. The high dust aerosol loading regions show significant negative radiative forcing. It indicates that the dust aerosol loading is negatively correlated with the DRE_{dust} in these dust storm events. The distribution maps of the LSA and the SZA (Fig. 3) show that the mean SW LSA measured by MODIS is around 0.18 and the mean SZA is around 35 degrees in Tamanrasset and Kashi. The distribution maps also show that the LSA and SZA vary greatly in the same satellite scan image. To avoid the influence of the LSA and SZA in estimating the $DRFE_{dust}$,

https://doi.org/10.5194/acp-2020-1113
Preprint. Discussion started: 14 January 2021

pixels with LSA of 0.16–0.20 and SZA of 32–38 degrees are chosen to derive the $DRFE_{dust}$. Therefore, only few pixels having similar values of the LSA and the SZA over Tamanrasset and Kashi are picked for estimating the DRE_{dust} and the $DRFE_{dust}$. The influences of the dust microphysical properties on the $DRFE_{dust}$ are investigated. These pixels of the DRE_{dust} and its co-located AOD values are illustrated in Table 1.

Table 1: DRE_{dust} and AOD in March 2019 over Tamanrasset and that in April 2019 over Kashi during the dust storms.

Regions & Dates \ Properties		AOD	DRE_{dust}
	20190309	0.92	-41.2
		1.51	-63.7
		1.11	-57.8
		0.31	-15.6
Sahara Desert	20190311	0.48	-11.5
		1.41	-43.5
		0.87	-36.7
	20190314	1.14	-44.6
		0.15	-5.8
	20190409	0.31	-12.3
		0.72	-39.5
		0.88	-35.4
	20190423	0.21	-8.3
Taklimakan Desert		0.35	-35.7
		0.11	-4.5
	20190425	0.79	-44.8
		0.98	-52.4
		0.55	-29.1

https://doi.org/10.5194/acp-2020-1113
Preprint. Discussion started: 14 January 2021

According to the definition, the $DRFE_{dust}$ represents the DRE_{dust} of a certain AOD at per unit area during these storms in the desert dust source regions. Therefore, the $DRFE_{dust}$ can be estimated by fitting the DRE_{dust} and the AOD.

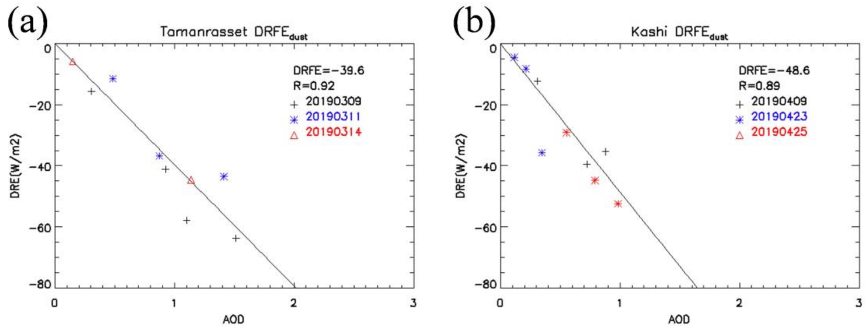

Figure 8: DRE_{dust} in (a) March 2019 over Tamanrasset and (b) April 2019 over Kashi.

The linear relationship between the DRE_{dust} and the AOD can be found during dust storms around Tamanrasset and Kashi, which is also investigated in previous studies (Kumar et al. 2015; Jose et al. 2016). Then, the $DRFE_{dust}$ can be estimated by regressing the DRE_{dust} and the AOD. In Fig. 8, the mean $DRFE_{dust}$ of the dust storms is −39.6 $Wm^{-2}\tau^{-1}$ over Tamanrasset and −48.6 $Wm^{-2}\tau^{-1}$ over Tamanrasset. The correlation coefficients are high with R = 0.92 in March 2019 over Tamanrasset and R = 0.89 in April 2019 over Kashi. The AOD and DRE_{dust} values are well correlated. Positive dust AOD is associated with negative DRE_{dust}.

The equi-albedo method directly estimates the DRE_{dust} and the $DRFE_{dust}$ based on the satellite observations. Therefore, the accuracy of the results (DRE_{dust} and $DRFE_{dust}$) derived from the equi-albedo method is highly dependent on the accuracy of satellite observations. Therefore, the uncertainties of the $DRFE_{dust}$ derived from the equi-albedo method mainly include the instantaneous SW flux error from CERES measurements, the estimation uncertainties of the F_{clr} over the dust storm region, and the uncertainty in the deep blue AOD product. Beside that, according to our sensitivity test in the previous studies (Tian et al., 2019), the atmospheric profile, water vapor and height of dust layer have insignificant influence on SW radiative flux at the TOA. It is reasonable to use same water vapor and pre-defined vertical distribution for dust aerosols in one scene of satellite data. However, the assumption of pixels has same water vapor and pre-defined aerosol vertical distribution over one scene of satellite data still cause small uncertainty.

https://doi.org/10.5194/acp-2020-1113
Preprint. Discussion started: 14 January 2021

Atmospheric Chemistry and Physics
Open Access
EGU
Discussions

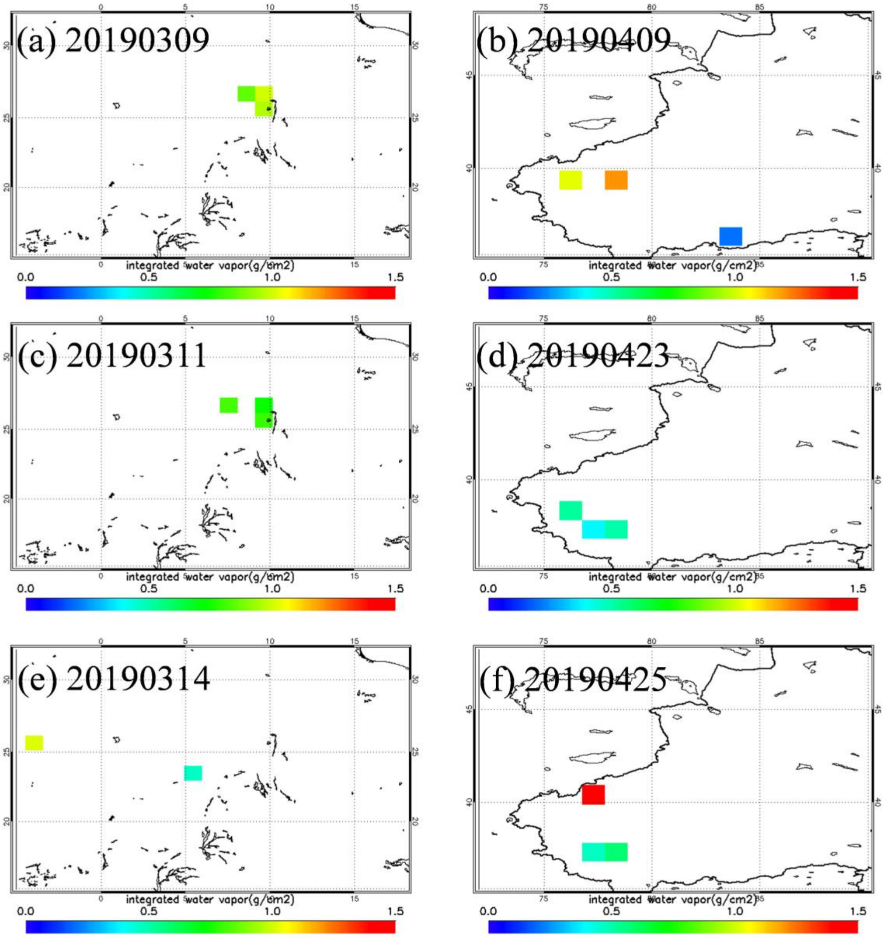

Figure 9: Integrated water vapor (g/cm^2) from European Centre for Medium-range Weather Forecasts (ECMWF) reanalyses dataset on March 2019 over Tamanrasset and on April 2019 over Kashi.

Fig.9 shows integrated water vapor from ECMWF reanalyses dataset on March 2019 over Tamanrasset and on April 2019 over Kashi. The integrated water vapor varies little over research areas, the regional mean differences are 0.51g/cm^2 and 0.18g/cm^2 over Kashi and Tamanrasset, respectively. In order to test the uncertainty caused by the varies of integrated water vapor over research areas, we calculated SW radiative flux at the TOA in difference of integrated water vapor based on SBDART model.

https://doi.org/10.5194/acp-2020-1113
Preprint. Discussion started: 14 January 2021

Atmospheric Chemistry and Physics
Discussions

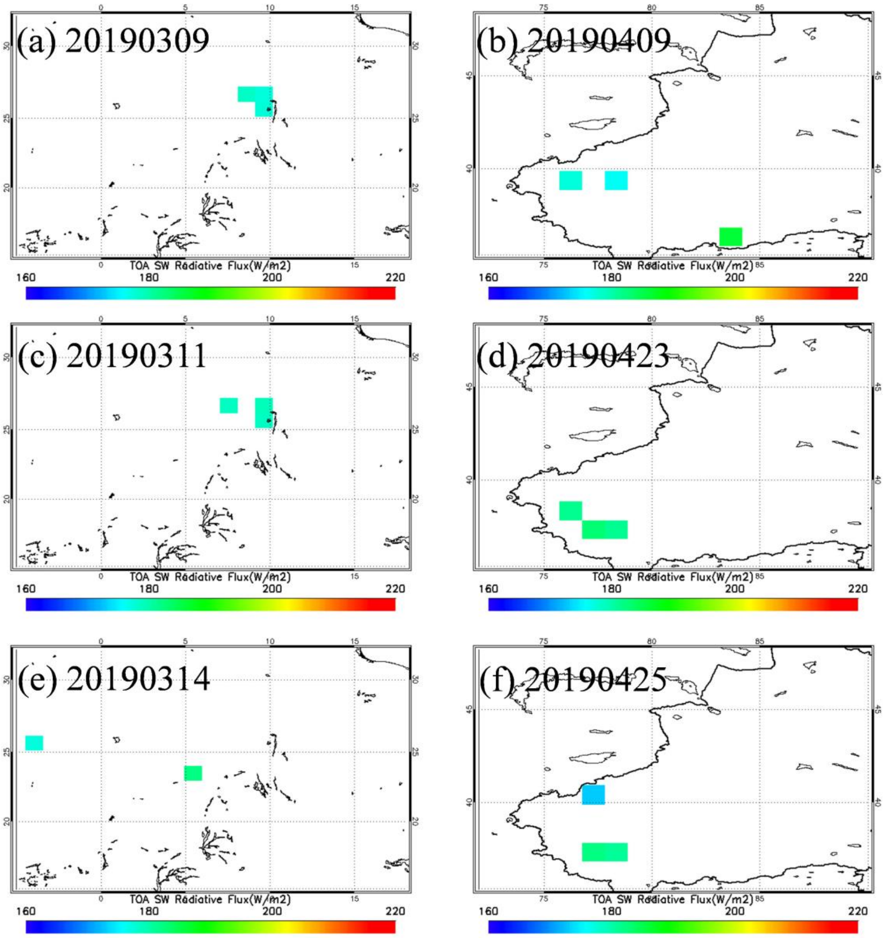

Figure 10: SBDART simulated clear-sky TOA radiative flux using integrated water vapor (g/cm2) from ECMWF reanalyses dataset on March 2019 over Tamanrasset and on April 2019 over Kashi.

Fig.10 shows SBDART simulated clear-sky TOA radiative flux using integrated water vapor from ECMWF reanalyses dataset on March 2019 over Tamanrasset and on April 2019 over Kashi. The regional mean differences of TOA radiative flux are 2.21% and 0.85% over Kashi and Tamanrasset, respectively. This indicates the varies of integrated water vapor caused uncertainties of TOA radiative flux are 2.21% and 0.85% over Kashi and Tamanrasset.

For the assumption of vertical profile for dust aerosols, we also tested the sensitivity of radiative flux at the top of atmosphere to changes height of dust layer with SBDART model.

https://doi.org/10.5194/acp-2020-1113
Preprint. Discussion started: 14 January 2021

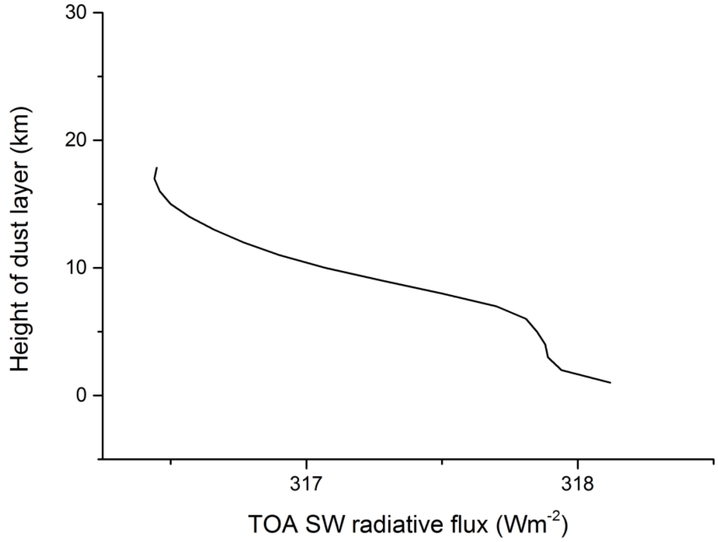

Figure 11: The sensitivity test of SW radiative flux at the TOA to changes height of dust layer.

As Fig.11 shown, the SW radiative flux at the TOA was decreased with the height of dust layer was increased from 0km to 18km. However, the contents of the SW radiative flux change little with the height of dust layer increased (within 1.5Wm^{-2}, 0.47%), which is little than CERES observation errors.

According to our previous study (Tian et al., 2019), the instantaneous SW flux error from CERES measurements is about 3.13%, the estimation uncertainty of the F_{clr} is 3.15%, the uncertainty of the deep blue AOD retrieved by MODIS is about 15% (Sayer et al., 2014), and the uncertainties of using same water vapor (2.21% and 0.85% over Kashi and Tamanrasset, respectively) and pre-defined aerosol vertical distribution (0.47%) over one scene of satellite data. Then, the total uncertainties of the $\mathrm{DRFE_{dust}}$ can be calculated by the equation Eq. (3) (Zhang et al., 2005).

$$U_t = \exp[\sum(logU_s)^2]^{1/2} \quad (3).$$

U_s is the synthetical uncertainty factor of each source of the uncertainty (including the instantaneous SW flux error from CERES measurements, the estimation uncertainty of the F_{clr}, and the uncertainty of the deep blue AOD retrieved by MODIS). U_t is the total uncertainty of the $\mathrm{DRFE_{dust}}$, which is 25.37% and 28.19% (10.0 Wm$^{-2}\tau^{-1}$ and 13.7 Wm$^{-2}\tau^{-1}$) in Tamanrasset and Kashi, respectively. Therefore, the $\mathrm{DRFE_{dust}}$ are −39.6 ± 10.0 Wm$^{-2}\tau^{-1}$ in March 2019 over Tamanrasset and −48.6 ± 13.7 Wm$^{-2}\tau^{-1}$ in April 2019 over Kashi.

https://doi.org/10.5194/acp-2020-1113
Preprint. Discussion started: 14 January 2021

Atmospheric Chemistry and Physics
Discussions

4 Deriving $DRFE_{dust}$ from the RTM simulations

4.1 Dust microphysical properties

The focuses of this paper are the differences in the dust microphysical properties from different dust source regions and the impacts of the dust microphysical properties on the $DRFE_{dust}$ simulation. As important parameters concerning the radiative impacts, the volume size distribution and the refractive index of the dust aerosol are compared in the dust storms over Tamanrasset and Kashi detected by MODIS.

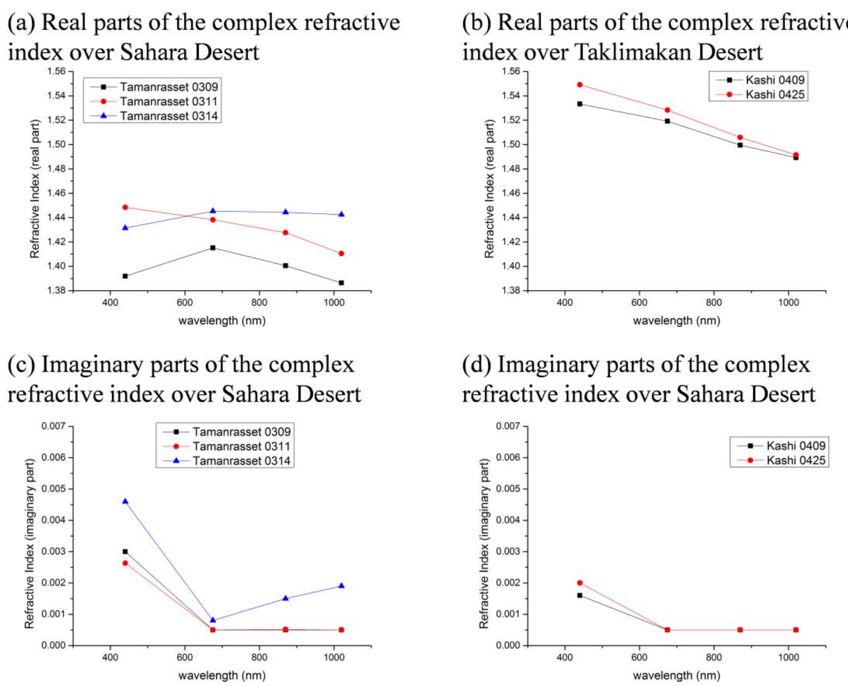

Figure 12: Real and imaginary parts of the dust complex refractive index from the Sahara Desert and the Taklimakan Desert.

The refractive index is a measurement of the aerosol refraction and absorption efficiency. Aerosols with high real parts of the complex refractive index values are indicated to be scattering types. Conversely, aerosols with high imaginary parts are indicated to be absorbing types (Zhang et al., 2006). Figure 12 shows the real and imaginary parts of the dust complex refractive index from the Taklimakan Desert and the Sahara Desert during the dust storms. In Fig. 12, dust aerosols from the Taklimakan desert (Fig. 12 (b)) have higher real parts and lower imaginary parts (Fig. 12 (d)) than the Sahara desert

https://doi.org/10.5194/acp-2020-1113
Preprint. Discussion started: 14 January 2021

(Fig. 12 (a) and Fig. 12 (c)), showing that the dust aerosols from the Taklimakan Desert have stronger scattering effects.

The volume size distribution of dust aerosols clearly shows the particle size difference between dusty and clear-sky days. The moderate and coarse aerosol particles with a radius within 0.5–10 μm show a significant increase under dusty conditions than those under non-dusty days. It is indicated that the quantity of the coarse mineral dust particles increases because of the dust storms. Figure 13 illustrates the variation of the dust aerosol size distribution during the dust storms in March 2019 over Tamanrasset and in April 2019 over Kashi. Most maximum dust aerosol size distribution peaks at the radius of 1.71 in Tamanrasset and 2.24 in Kashi. Moreover, the peak values are higher in Kashi. It is indicated that the dust storm is stronger in April 2019 over Kashi and the coarse mode aerosol particles increase in particle volume compared with those in the dust storm in March 2019 over Tamanrasset.

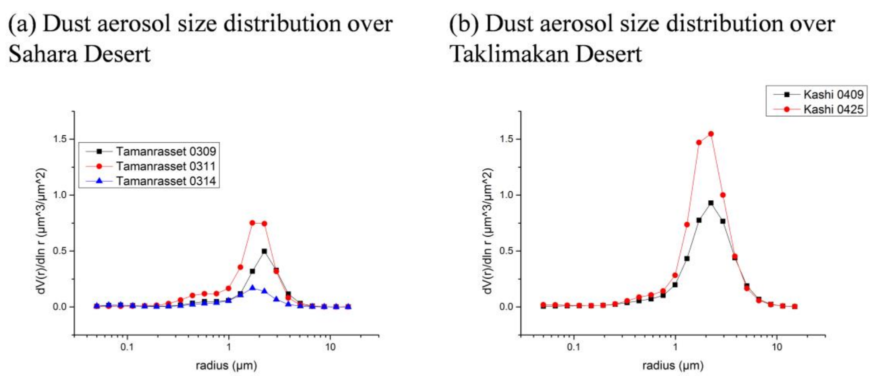

Figure 13: Dust aerosol size distribution over (a) the Sahara Desert and (b) the Taklimakan Desert.

4.2 Dust optical properties

The dust optical properties can be calculated by synergistically using the real and imaginary parts of the dust complex refractive index and the dust aerosol size distribution.

The SSA and the ASY are two key parameters determining the DRE_{dust} and the $DRFE_{dust}$. Accurate measurements of the SSA and the ASY are important for the assessment of the direct effect of aerosols on climate (Qie et al., 2019). The dust aerosol optical properties are calculated by using the Mie theory, the T-matrix method, and the AERONET inversion products (Dubovik and King, 2000;Dubovik et al., 2006).

The SSA is presented as the ratio between the aerosol scattering and extinction coefficients. The dust SSA describes the scattering properties of the dust aerosols. The SSA can largely determine the magnitudes and signs of the DRE_{dust} and the $DRFE_{dust}$. Strongly scattering dust aerosols (i.e., SSA = 1) always cause negative DRE_{dust}. By contrast, low SSA aerosols often cause positive DRE_{dust}, especially over high LSA regions as the light absorbed by the aerosols can reduce the cooling effect. A high SSA is correlated with low real parts of the complex refractive index, while a strong absorption is correlated with a high imaginary part of the complex refractive index. Together with the size distribution, real parts of the complex refractive index can determine the magnitude of the SSA.

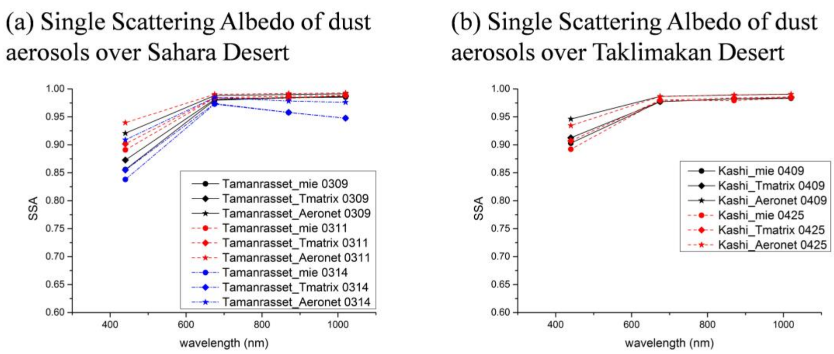

Figure 14: Single scattering albedo from (a) the Sahara Desert and (b) the Taklimakan Desert..

Figure 14 shows the variabilities of the dust aerosol SSA between different dust source regions and different calculation methods. In Fig. 14, the maximum SSA value mostly occurs at the wavelength of 1020 nm, which indicates that the SSA is dependent on wavelength. Moreover, dust aerosols from the Taklimakan desert (Kashi) in the figure have higher SSA value using both the Mie theory and the T-matrix method. The higher value of SSA shows that dust aerosol particles scatter more predominantly and strongly in the Taklimakan desert (Kashi), which may cause more significant negative radiative forcing than the dust aerosols from the Sahara Desert (Tamanrasset).

https://doi.org/10.5194/acp-2020-1113
Preprint. Discussion started: 14 January 2021

Atmospheric Chemistry and Physics Discussions

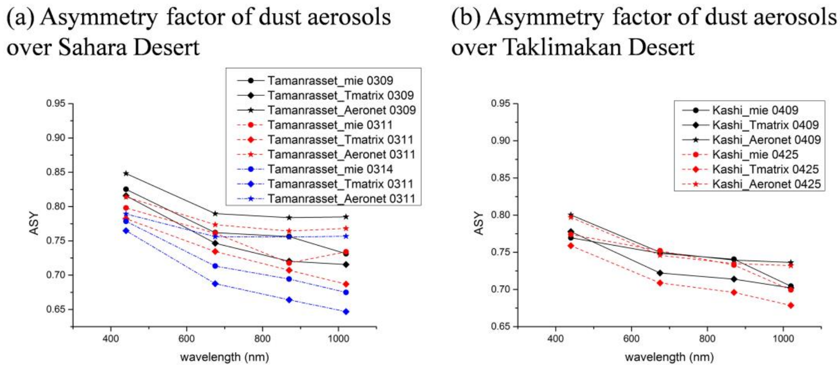

Figure 15: Asymmetry factor in (a) the Sahara Desert and (b) the Taklimakan Desert.

The ASY indicates the relative strength of the forward scattering, which determines the integrated fractions of the energy that scatter backward and forward. The dust aerosol particles with sharp peaks in the forward direction (0 ° scattering angle) have positive ASY. The ASY value increases with the particle size.

The ASY in Fig. 15 shows marked spectral variation with higher values at shorter wavelengths. It can be found that the dust aerosols from the Sahara Desert (Tamanrasset) have higher values of the ASY than those from the Taklimakan desert (Kashi) in both the Mie theory and the T-matrix method. The high values (over 0.80 at 440 nm) reflect the dominance of the absorbing of dust aerosols. The stronger backward scattered energy may cause higher negative radiative forcing in the Taklimakan Desert (Kashi).

According to the analyses of the microphysical properties and the optical properties, the dust aerosols from the Taklimakan Desert (Kashi) scatter strongly. The negative $DRFE_{dust}$ from the Taklimakan desert (Kashi) should be more significant than those from the Sahara Desert (Tamanrasset). The results are in good agreement with those estimated by the satellite observations.

https://doi.org/10.5194/acp-2020-1113
Preprint. Discussion started: 14 January 2021

Atmospheric Chemistry and Physics
Discussions

4.3 DRFE$_{dust}$ derived from the RTM simulations

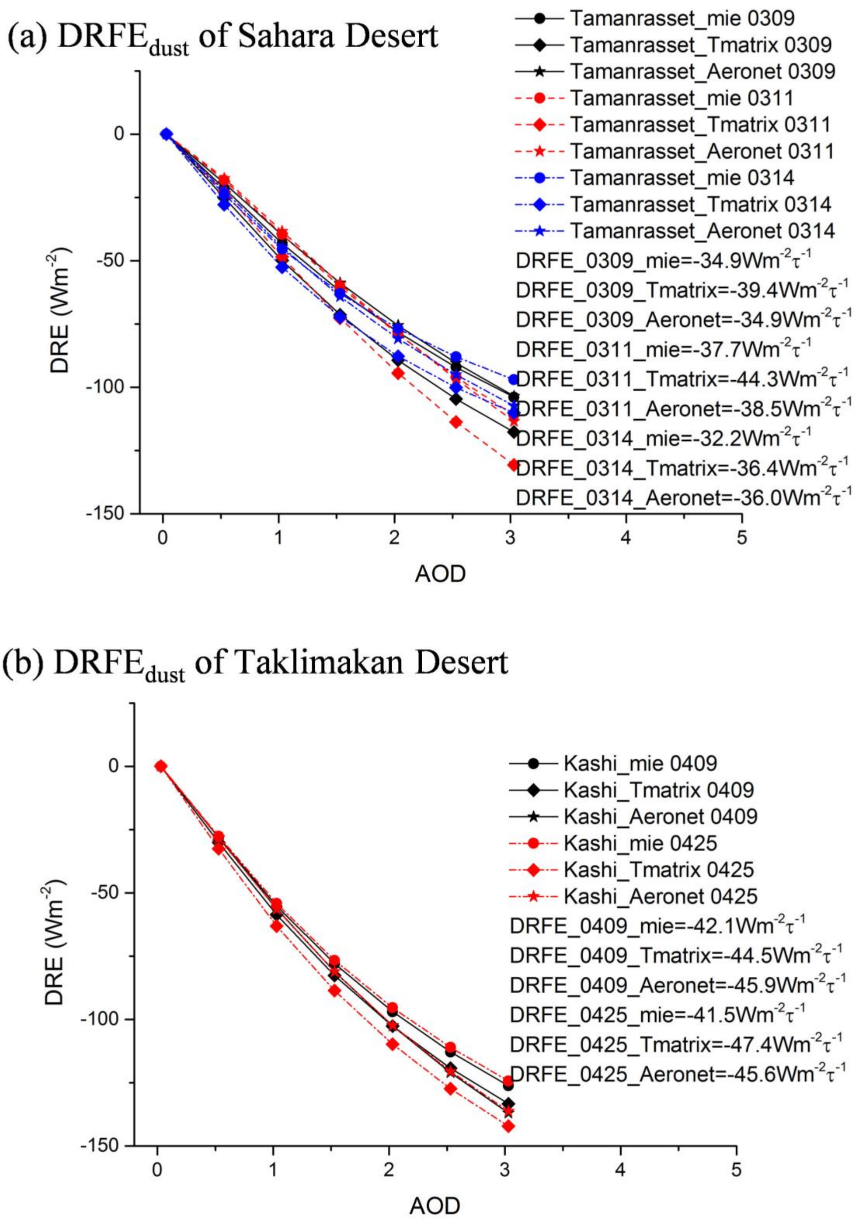

Figure 16: DRFE$_{dust}$ simulated by the SBDART in (a) Tamanrasset and (b) Kashi.

The DRFE$_{dust}$ estimated directly by the satellite observation is compared with that simulated by the SBDART to verify the reliability. As shown in Fig. 16, with higher aerosol scattering (higher SSA) and

https://doi.org/10.5194/acp-2020-1113
Preprint. Discussion started: 14 January 2021

higher backward scattering coefficients (lower ASY), the negative $DRFE_{dust}$ from Kashi is more significant. The mean $DRFE_{dust}$ from Kashi is -37.1 W m^{-2} τ^{-1}. The dust aerosols from Kashi have stronger cooling effects than those from Tamanrasset, in which the mean $DRFE_{dust}$ is -44.5 W m^{-2} τ^{-1}. The results are in good agreement with those estimated by the satellite observations. The $DRFE_{dust}$ estimated by the dust optical properties derived from the T-matrix method and the AERONET is closer to those estimated by the satellite observations, which indicates that most dust aerosols are non-spherical in the natural environment.

The results also show that the dust microphysical properties can significantly influence the $DRFE_{dust}$. The mean difference of the $DRFE_{dust}$ between Tamanrasset and Kashi is 9.0% (7.4 W m^{-2} τ^{-1}). Even for the same dust microphysical property, the $DRFE_{dust}$ varies significantly according to whether the dust particles are considered spherical or non-spherical in different methods. For the differences of the $DRFE_{dust}$ estimated using different methods, the mean standard deviations are 7.6% (2.8 W m^{-2} τ^{-1}) in Tamanrasset and 6.8% (3.0 W m^{-2} τ^{-1}) in Kashi. Moreover, Li et al. (2020) pointed out that the atmospheric profile, LSA and SZA, can also influence the simulation of the instantaneous $DRFE_{dust}$, which agrees with our previous study (Tian et al., 2019). Additionally, it is difficult for climate models or in-situ measurements to get the real distribution of the aerosol properties at a large spatial extent. Also, it is hard to evaluate the uncertainties in radiative transfer simulations. It can cause significant errors in evaluating the modulating effects of the mineral dust aerosols on climate (Huang et al., 2009;Li et al., 2020).

5 $DRFE_{dust}$ in the satellite-based observation and the simulation of the RTM

According to the analyses of the dust aerosol microphysical properties and optical properties, the dust aerosols from the Taklimakan Desert (Kashi) should scatter strongly. The RTM simulation results are in good agreement with the results estimated by the satellite observation. Previous studies also estimated the $DRFE_{dust}$ in the Sahara Desert and the Taklimakan Desert (Li et al., 2020;Li et al., 2004;García et al., 2012;Xia and Zong, 2009), which validate our results.

Table 2: SW $DRFE_{dust}$ from different studies.

Dust source regions	Research	Model/Method	$DRFE_{dust}$ ($Wm^{-2}\tau^{-1}$)	Description
Sahara	García et al	Ground+GAM	~ -35	AERONET

Desert	(2012)	E		$DRFE_{dust}$ in December-January -February, with LSA<0.3.
	Li et al (2004)	Satellite+SBDART	-35±3 (summer) -26±3 (winter)	Binned mean fitting TOA diurnal mean $DRFE_{dust}$ over the Atlantic Ocean near the African coast.
	This paper	Satellite Satellite+SBDART	-39.6±10.0 (Satellite) -32.2 ~ -44.3 (SBDART)	
Taklimakan Desert	Li et al (2020)	Ground+SBDART	-45~-50	Instantaneous $DRFE_{dust}$ at 04:08 UTC.
	García et al (2012)	Ground+GAME	~ -45	AERONET $DRFE_{dust}$ in March-April-May, with LSA<0.3.
	Xia and Zong (2009)	Satellite + SBDART	-48.1	Instantaneous $DRFE_{dust}$ at about 05:00 UTC.
	This paper	Satellite Satellite+SBDART	-48.6±13.7 (Satellite) -41.5 ~ -47.4 (SBDART)	

Table 2 illustrates the SW $DRFE_{dust}$ of the Sahara Desert and the Taklimakan Desert in previous studies. García et al. (2012) evaluated the $DRFE_{dust}$ based on the GAME model and the AERONET retrievals, which indicated that the mean $DRFE_{dust}$ is around -35 W m^{-2} τ^{-1} in the Sahara Desert and -45 W m^{-2} τ^{-1} in the Taklimakan Desert in similar observational conditions (i.e., for the SZA between 55° and 65°, for the LSA below 0.3). Li et al. (2004) estimated the diurnal mean $DRFE_{dust}$ at the TOA (-35 ± 3 W m^{-2} τ^{-1} in summer; -26 ± 3 W m^{-2} τ^{-1} in winter) over the Atlantic Ocean near the African coast. The results indicated that lower uncertainties are derived from the standard deviation of the best-fit curve around the observed points due to the binned mean fitting. For the Taklimakan Desert, Li et al. (2020) estimated the instantaneous SW $DRFE_{dust}$ at 04:08 UTC (around -43 W m^{-2} τ^{-1}) at the TOA of Kashi on 25 April 2019. In this paper, the $DRFE_{dust}$ of the Taklimakan Desert is estimated with the same dust properties referring to the works of Li et al. (2020). Furthermore, Xia and Zong (2009) used both the satellite data and the SBDART model to represent the instantaneous (about 05:00 UTC) SW $DRFE_{dust}$, which is −48.1 W m^{-2} τ^{-1} at the TOA(Xia and Zong, 2009). Through comparison, it is found that the satellite-based equi-albedo method and the SBDART model-derived SW $DRFE_{dust}$ are −39.6 ± 10.0 W m^{-2} τ^{-1} and −32.2 to −44.3 W m^{-2} τ^{-1} at the TOA over the Sahara Desert, respectively, which are −48.6 ± 13.7 W m^{-2} τ^{-1} and −41.5 to −47.4 W m^{-2} τ^{-1} at the TOA over the Taklimakan Desert, respectively. The methods and results in these studies are comparable despite the differences. The results show that the negative $DRFE_{dust}$ from the Taklimakan Desert is more significant than those from the Sahara Desert. As the SZA and LSA variations are considered in these studies, the results in this paper are reasonable and reliable. The compared results show that the $DRFE_{dust}$ derived from the satellite-based equi-albedo method is closer to that in previous studies with lower uncertainty. The $DRFE_{dust}$ estimated by the satellite-based equi-albedo method is obtained without the dust microphysical properties being assumed. The uncertainties are mostly caused by observation errors. Therefore, the uncertainties can be evaluated more reasonably. It provides a direct way to validate the DRE_{dust} and the $DRFE_{dust}$.

6 Discussion and conclusions

This study analyzes the differences in the dust microphysical properties and the $DRFE_{dust}$ over the Taklimakan Desert and the Sahara Desert during dust storms. The satellite-based equi-albedo method and the RTM are both used to estimate the $DRFE_{dust}$ in this study. By comparing the results from different methods and dust source regions, the $DRFE_{dust}$ differences caused by dust microphysical properties and particle shapes are discussed.

The results show that the dust aerosols from the Taklimakan Desert have higher aerosol scattering (higher SSA) and backward scattering coefficients (lower ASY), and it causes more significant negative $DRFE_{dust}$ (−48.6 ± 13.7 W m^{-2} τ^{-1} by the satellite; −41.5 to −47.4 W m^{-2} τ^{-1} by the SBDART) than that in the Sahara Desert (−39.6 ± 10.0 W m^{-2} τ^{-1} by the satellite; −32.2 to −44.3 W m^{-2} τ^{-1} by the SBDART). It is indicated that the dust microphysical properties and particle shapes can significantly influence on the $DRFE_{dust}$. The information on the accurate dust microphysical properties and dust origins is highly required in the $DRFE_{dust}$ simulation. The scant measurements on dust microphysical properties can cause large uncertainties in simulating the $DRFE_{dust}$. Previous studies proved that the

https://doi.org/10.5194/acp-2020-1113
Preprint. Discussion started: 14 January 2021

Atmospheric Chemistry and Physics Discussions

results in this paper are reasonable and reliable. The $DRFE_{dust}$ derived from the satellite-based equi-albedo method is close to the results in previous studies.

However, there are still uncertainties in the simulation of the $DRFE_{dust}$. In contrast, the $DRFE_{dust}$ can be estimated directly from the satellite observation using the equi-albedo method without any assumptions of the microphysical properties of dust aerosols. It has unique advantages in estimating the $DRFE_{dust}$. Also, it can validate the DRE_{dust} and the $DRFE_{dust}$ derived from the numerical models more directly.

Data availability

The CERES data can be accessed from the Atmospheric Sciences Data Center of NASA Langley Research Center (https://ceres.larc.nasa.gov/order_data.php). The AQUA/MODIS aerosol Products (MYD04_L2) can be accessed from the NASA Level-1 and Atmosphere Archive and Distribution System (LAADS) Distributed Active Archive Center (DAAC) website (https://ladsweb.modaps.eosdis.nasa.gov/). The MODIS albedo products (MCD43C3 Version 6) can be accessed from the NASA LP DAAC website (https://lpdaac.usgs.gov/tools/data-pool/). The AERONET data were obtained from the AERONET website (http://aeronet.gsfc.nasa.gov).

Author contributions

PZ and LC designed the study, and LT performed the study with suggestions from PZ and LC. LB improved the scattering calculating method of dust particles. Both authors contributed to the writing of this article.

Competing interests

The authors declare that they have no conflict of interest.

Special issue statement

This article is part of the special issue "Satellite and ground-based remote sensing of aerosol optical, physical, and chemical properties over China". It is not associated with a conference.

https://doi.org/10.5194/acp-2020-1113
Preprint. Discussion started: 14 January 2021

Acknowledgments

We acknowledge the groups of MODIS, CERES, ECMWF, and AERONET for providing the AOD, LSA, integrated water vapor, aerosol microphysical, and optical properties products. We also thank the SBDART group for making SBDART available. We thank Nanjing Hurricane Translation for reviewing the English language quality of this paper.

Financial support

This work was funded by the National Key R&D Program of China (grant number 2018YFB0504900 and 2018YFB0504905), National Natural Science Foundation (grant number 41675036).

References

Anderson, T. L., Charlson, R. J., Bellouin, N., Boucher, O., Chin, M., Christopher, S. A., Haywood, J., Kaufman, Y. J., Kinne, S., Ogren, J. A., Remer, L. A., Takemura, T., Tanré, D., Torres, O., Trepte, C. R., Wielicki, B. A., Winker, D. M., and Yu, H.: An "A-Train" Strategy for Quantifying Direct Climate Forcing by Anthropogenic Aerosols, Bulletin of the American Meteorological Society, 86, 1795-1810, 10.1175/bams-86-12-1795, 2005.

Bi, J., Shi, J., Xie, Y., Liu, Y., Takamura, T., and Khatri, P.: Dust Aerosol Characteristics and Shortwave Radiative Impact at a Gobi Desert of Northwest China during the Spring of 2012, Journal of the Meteorological Society of Japan. Ser. II, 92A, 33-56, 10.2151/jmsj.2014-A03, 2014.

Bi, L., Ding, S., Zong, R., and Yi, B.: Examining Asian dust refractive indices for brightness temperature simulations in the 650–1135 cm−1 spectral range, Journal of Quantitative Spectroscopy and Radiative Transfer, 247, 106945, https://doi.org/10.1016/j.jqsrt.2020.106945, 2020.

Borghese, F., Denti, P., Saija, R., and Iatì, M. A.: Optical trapping of nonspherical particles in the T-matrix formalism, Opt. Express, 15, 11984-11998, 10.1364/OE.15.011984, 2007.

Che, H., Zhang, X., Alfraro, S., Chatenet, B., Gomes, L., and Zhao, J.: Aerosol optical properties and its radiative forcing over Yulin, China in 2001 and 2002, Advances in Atmospheric Sciences, 26, 564-576, 10.1007/s00376-009-0564-4, 2009.

Che, H., Wang, Y., Sun, J., Zhang, X., Zhang, X., and Guo, J.: Variation of Aerosol Optical Properties over Taklimakan Desert of China, Aerosol and Air Quality Research, 13, 777-785, 10.4209/aaqr.2012.07.0200, 2012.

Chen, L., Shi, G., Qin, S., Yang, S., and Zhang, P.: Direct radiative forcing of anthropogenic aerosols over oceans from satellite observations, Advances in Atmospheric Sciences, 28, 973-984, 10.1007/s00376-010-9210-4, 2011.

Christopher, S. A., Chou, J., Zhang, J., Li, X., Berendes, T. A., and Welch, R. M.: Shortwave direct radiative forcing of biomass burning aerosols estimated using VIRS and CERES data, Geophysical Research Letters, 27, 2197-2200, 10.1029/1999gl010923, 2000.

https://doi.org/10.5194/acp-2020-1113
Preprint. Discussion started: 14 January 2021

Atmospheric Chemistry and Physics Discussions

Chylek, P., Grams, G., and Pinnick, R.: Light Scattering by Nonspherical Particles, 82, 1977.

Colarco, P. R., Nowottnick, E. P., Randles, C. A., Yi, B., Yang, P., Kim, K.-M., Smith, J. A., and Bardeen, C. G.: Impact of radiatively interactive dust aerosols in the NASA GEOS-5 climate model: Sensitivity to dust particle shape and refractive index, Journal of Geophysical Research: Atmospheres, 119, 753-786, 10.1002/2013jd020046, 2014.

Di Biagio, C., di Sarra, A., Eriksen, P., Ascanius, S. E., Muscari, G., and Holben, B.: Effect of surface albedo, water vapour, and atmospheric aerosols on the cloud-free shortwave radiative budget in the Arctic, Climate Dynamics, 39, 953-969, 10.1007/s00382-011-1280-1, 2012.

Di Biagio, C., Boucher, H., Caquineau, S., Chevaillier, S., Cuesta, J., and Formenti, P.: Variability of the infrared complex refractive index of African mineral dust: Experimental estimation and implications for radiative transfer and satellite remote sensing, Atmospheric Chemistry and Physics, 14, 10.5194/acp-14-11093-2014, 2014a.

Di Biagio, C., Formenti, P., Styler, S. A., Pangui, E., and Doussin, J.-F.: Laboratory chamber measurements of the longwave extinction spectra and complex refractive indices of African and Asian mineral dust, Geophysical Research Letters, 41, 10.1002/2014GL060213, 2014b.

Di Biagio, C., Formenti, P., Balkanski, Y., Caponi, L., Cazaunau, M., Pangui, E., Journet, E., Nowak, S., Caquineau, S., Andreae, M. O., Kandler, K., Saeed, T., Piketh, S., Seibert, D., Williams, E., and Doussin, J. F.: Global scale variability of the mineral dust long-wave refractive index: a new dataset of in situ measurements for climate modeling and remote sensing, Atmos. Chem. Phys., 17, 1901-1929, 10.5194/acp-17-1901-2017, 2017.

Dubovik, O., and King, M. D.: A flexible inversion algorithm for retrieval of aerosol optical properties from Sun and sky radiance measurements, Journal of Geophysical Research: Atmospheres, 105, 20673-20696, 10.1029/2000jd900282, 2000.

Dubovik, O., Sinyuk, A., Lapyonok, T., Holben, B. N., Mishchenko, M., Yang, P., Eck, T. F., Volten, H., Muñoz, O., Veihelmann, B., van der Zande, W. J., Leon, J.-F., Sorokin, M., and Slutsker, I.: Application of spheroid models to account for aerosol particle nonsphericity in remote sensing of desert dust, Journal of Geophysical Research: Atmospheres, 111, 10.1029/2005jd006619, 2006.

Gao, Y., and Anderson, J. R.: Characteristics of Chinese aerosols determined by individual-particle analysis, Journal of Geophysical Research: Atmospheres, 106, 18037-18045, 10.1029/2000jd900725, 2001.

García, O. E., Díaz, A. M., Expósito, F. J., Díaz, J. P., Dubovik, O., Dubuisson, P., Roger, J.-C., Eck, T. F., Sinyuk, A., Derimian, Y., Dutton, E. G., Schafer, J. S., Holben, B. N., and García, C. A.: Validation of AERONET estimates of atmospheric solar fluxes and aerosol radiative forcing by ground-based broadband measurements, Journal of Geophysical Research: Atmospheres, 113, 10.1029/2008jd010211, 2008.

García, O. E., Díaz, J. P., Expósito, F. J., Díaz, A. M., Dubovik, O., Derimian, Y., Dubuisson, P., and Roger, J. C.: Shortwave radiative forcing and efficiency of key aerosol types using AERONET data, Atmos. Chem. Phys., 12, 5129-5145, 10.5194/acp-12-5129-2012, 2012.

Garrett, T. J., and Zhao, C.: Increased Arctic cloud longwave emissivity associated with pollution from mid-latitudes, Nature, 440, 787-789, 10.1038/nature04636, 2006.

Gouesbet, G., and Gréhan, G.: Generalized Lorenz-Mie Theories, 2011.

Guirado-Fuentes, C., Cuevas, E., Cachorro, V., Toledano, C., Alonso-Pérez, S., Bustos, J., Basart, S., Romero, P., Camino, C., Mimouni, M., Zeudmi, L., Goloub, P., Baldasano, J., and Frutos Baraja, A.: Aerosol characterization at the Saharan AERONET site Tamanrasset, Atmospheric Chemistry and

https://doi.org/10.5194/acp-2020-1113
Preprint. Discussion started: 14 January 2021

Atmospheric Chemistry and Physics Discussions

Physics, 14, 11753-11773, 10.5194/acp-14-11753-2014, 2014.

Hsu, N. C., Tsay, S. C., King, M. D., and Herman, J. R.: Aerosol properties over bright-reflecting source regions, IEEE Transactions on Geoscience & Remote Sensing, 42, 557-569, 2004.

Huang, J., Fu, Q., Su, J., and Tang, Q.: Taklimakan dust aerosol radiative heating derived from CALIPSO observations using the Fu-Liou radiation model with CERES constraints, Atmospheric Chemistry and Physics Discussions, 2009.

Huang, J., Wang, T., Wang, W., Li, Z., and Yan, H.: Climate effects of dust aerosols over East Asian arid and semiarid regions, Journal of Geophysical Research: Atmospheres, 119, 11,398-311,416, 10.1002/2014jd021796, 2014.

Huneeus, N., Chevallier, F., and Boucher, O.: Estimating aerosol emissions by assimilating observed aerosol optical depth in a global aerosol model, Atmospheric Chemistry & Physics, 12, 4585-4606, 10.5194/acp-12-4585-2012, 2012.

Iftikhar, M., Alam, K., Sorooshian, A., Syed, W. A., Bibi, S., and Bibi, H.: Contrasting aerosol optical and radiative properties between dust and urban haze episodes in megacities of Pakistan, Atmospheric Environment, 173, 157-172, https://doi.org/10.1016/j.atmosenv.2017.11.011, 2018.

Jin, Y., Schaaf, C. B., Woodcock, C. E., Gao, F., Li, X., Strahler, A. H., Lucht, W., and Liang, S.: Consistency of MODIS surface bidirectional reflectance distribution function and albedo retrievals: 2. Validation, Journal of Geophysical Research: Atmospheres, 108, 10.1029/2002jd002804, 2003.

Kalashnikova, O. V., and Sokolik, I. N.: Modeling the radiative properties of nonspherical soil-derived mineral aerosols, Journal of Quantitative Spectroscopy and Radiative Transfer, 87, 137-166, https://doi.org/10.1016/j.jqsrt.2003.12.026, 2004.

Li, F., Vogelmann, A. M., and Ramanathan, V.: Saharan Dust Aerosol Radiative Forcing Measured from Space, Journal of Climate, 17, 2558-2571, 10.1175/1520-0442(2004)017<2558:SDARFM>2.0.CO;2, 2004.

Li, L., Li, Z., Chang, W., Ou, Y., Goloub, P., Li, C., Li, K., Hu, Q., Wang, J., and Wendisch, M.: Solar radiative forcing of aerosol particles near the Taklimakan desert during the Dust Aerosol Observation-Kashi campaign in Spring 2019, Atmos. Chem. Phys. Discuss., 2020, 1-29, 10.5194/acp-2020-60, 2020.

Li, Z. Q., Xu, H., Li, K. T., Li, D. H., Xie, Y. S., Li, L., Zhang, Y., Gu, X. F., Zhao, W., Tian, Q. J., Deng, R. R., Su, X. L., Huang, B., Qiao, Y. L., Cui, W. Y., Hu, Y., Gong, C. L., Wang, Y. Q., Wang, X. F., Wang, J. P., Du, W. B., Pan, Z. Q., Li, Z. Z., and Bu, D.: Comprehensive Study of Optical, Physical, Chemical, and Radiative Properties of Total Columnar Atmospheric Aerosols over China: An Overview of Sun–Sky Radiometer Observation Network (SONET) Measurements, Bulletin of the American Meteorological Society, 99, 739-755, 10.1175/bams-d-17-0133.1, 2018.

Liang, S., Fang, H., Chen, M., Shuey, C. J., Walthall, C., Daughtry, C., Morisette, J., Schaaf, C., and Strahler, A.: Validating MODIS land surface reflectance and albedo products: methods and preliminary results, Remote Sensing of Environment, 83, 149-162, https://doi.org/10.1016/S0034-4257(02)00092-5, 2002.

Liu, J., Schaaf, C., Strahler, A., Jiao, Z., Shuai, Y., Zhang, Q., Roman, M., Augustine, J. A., and Dutton, E. G.: Validation of Moderate Resolution Imaging Spectroradiometer (MODIS) albedo retrieval algorithm: Dependence of albedo on solar zenith angle, Journal of Geophysical Research: Atmospheres, 114, 10.1029/2008jd009969, 2009.

Mbourou, G. N. T., Bertrand, J. J., and Nicholson, S. E.: The Diurnal and Seasonal Cycles of Wind-Borne Dust over Africa North of the Equator, Journal of Applied Meteorology, 36, 868-882, 10.1175/1520-0450(1997)036<0868:Tdasco>2.0.Co;2, 1997.

Mikami, M., Shi, G. Y., Uno, I., Yabuki, S., Iwasaka, Y., Yasui, M., Aoki, T., Tanaka, T. Y., Kurosaki, Y., Masuda, K., Uchiyama, A., Matsuki, A., Sakai, T., Takemi, T., Nakawo, M., Seino, N., Ishizuka, M., Satake, S., Fujita, K., Hara, Y., Kai, K., Kanayama, S., Hayashi, M., Du, M., Kanai, Y., Yamada, Y., Zhang, X. Y., Shen, Z., Zhou, H., Abe, O., Nagai, T., Tsutsumi, Y., Chiba, M., and Suzuki, J.: Aeolian dust experiment on climate impact: An overview of Japan–China joint project ADEC, Global and Planetary Change, 52, 142-172, https://doi.org/10.1016/j.gloplacha.2006.03.001, 2006.

Miller, R., Knippertz, P., Pérez García-Pando, C., Perlwitz, J., and Tegen, I.: Impact of Dust Radiative Forcing upon Climate, in, 327-357, 2014.

Mishchenko, M. I., Travis, L. D., and Mackowski, D. W.: T-matrix computations of light scattering by nonspherical particles: A review, Journal of Quantitative Spectroscopy and Radiative Transfer, 55, 535-575, https://doi.org/10.1016/0022-4073(96)00002-7, 1996.

Mishchenko, M. I., and Travis, L. D.: Capabilities and limitations of a current FORTRAN implementation of the T-matrix method for randomly oriented, rotationally symmetric scatterers, Journal of Quantitative Spectroscopy and Radiative Transfer, 60, 309-324, https://doi.org/10.1016/S0022-4073(98)00008-9, 1998.

Mishchenko, M. I., and Travis, L. D.: Gustav Mie and the Evolving Discipline of Electromagnetic Scattering by Particles, Bulletin of the American Meteorological Society, 89, 1853-1862, 10.1175/2008bams2632.1, 2008.

Nakajima, T., Tanaka, M., Yamano, M., Shiobara, M., Arao, K., and Nakanishi, Y.: Aerosol Optical Characteristics in the Yellow Sand Events Observed in May, 1982 at Nagasaki-Part II Models, Journal of the Meteorological Society of Japan. Ser. II, 67, 279-291, 10.2151/jmsj1965.67.2_279, 1989.

Okada, K., Heintzenberg, J., Kai, K., and Qin, Y.: Shape of atmospheric mineral particles collected in three Chinese arid-regions, Geophysical Research Letters, 28, 3123-3126, 10.1029/2000gl012798, 2001.

Qie, L., Li, L., Li, K., Li, D., and Xu, H.: Retrieval of aerosol optical properties from ground-based remote sensing measurements: Aerosol asymmetry factor and single scattering albedo, 2019.

Ramanathan, V., Cess, R., Harrison, E., Minnis, P., Barkstrom, B., Ahmad, E., and Hartmann, D.: Cloud-Radiative Forcing and Climate: Results from The Earth Radiation Budget Experiment, Science (New York, N.Y.), 243, 57-63, 10.1126/science.243.4887.57, 1989.

Remer, L. A., Kaufman, Y. J., Tanré, D., Mattoo, S., Chu, D. A., Martins, J. V., Li, R. R., Ichoku, C., Levy, R. C., Kleidman, R. G., Eck, T. F., Vermote, E., and Holben, B. N.: The MODIS Aerosol Algorithm, Products, and Validation, Journal of the Atmospheric Sciences, 62, 947-973, 10.1175/JAS3385.1, 2005.

Ricchiazzi, P., Yang, S., Gautier, C., and Sowle, D.: SBDART: A Research and Teaching Software Tool for Plane-Parallel Radiative Transfer in the Earth's Atmosphere, Bulletin of the American Meteorological Society, 79, 2101-2114, 10.1175/1520-0477(1998)079<2101:Sarats>2.0.Co;2, 1998.

Román, M. O., Schaaf, C. B., Lewis, P., Gao, F., Anderson, G. P., Privette, J. L., Strahler, A. H., Woodcock, C. E., and Barnsley, M.: Assessing the coupling between surface albedo derived from MODIS and the fraction of diffuse skylight over spatially-characterized landscapes, Remote Sensing of Environment, 114, 738-760, https://doi.org/10.1016/j.rse.2009.11.014, 2010.

Satheesh, S. K., and Ramanathan, V.: Large differences in tropical aerosol forcing at the top of the atmosphere and Earth's surface, Nature, 405, 60-63, 10.1038/35011039, 2000.

Satheesh, S. K.: <i>Letter to the Editor</i>
Aerosol radiative forcing over land: effect of surface

https://doi.org/10.5194/acp-2020-1113
Preprint. Discussion started: 14 January 2021

Atmospheric Chemistry and Physics
Discussions

and cloud reflection, Ann. Geophys., 20, 2105-2109, 10.5194/angeo-20-2105-2002, 2002.

Satheesh, S. K., and Srinivasan, J.: A Method to Estimate Aerosol Radiative Forcing from Spectral Optical Depths, Journal of Atmospheric Sciences, 63, 1082, 10.1175/jas3663.1, 2006.

Sayer, A. M., Munchak, L. A., Hsu, N. C., Levy, R. C., Bettenhausen, C., and Jeong, M.-J.: MODIS Collection 6 aerosol products: Comparison between Aqua's e-Deep Blue, Dark Target, and "merged" data sets, and usage recommendations, Journal of Geophysical Research: Atmospheres, 119, 13,965-913,989, 10.1002/2014jd022453, 2014.

Schaaf, C., Martonchik, J., Pinty, B., Govaerts, Y., Gao, F., Lattanzio, A., Liu, J., Strahler, A., and Taberner, M.: Retrieval of Surface Albedo from Satellite Sensors, in: Advances in Land Remote Sensing: System, Modeling, Inversion and Application, edited by: Liang, S., Springer Netherlands, Dordrecht, 219-243, 2008.

Schaaf, C. B., Gao, F., Strahler, A. H., Lucht, W., Li, X., Tsang, T., Strugnell, N. C., Zhang, X., Jin, Y., Muller, J.-P., Lewis, P., Barnsley, M., Hobson, P., Disney, M., Roberts, G., Dunderdale, M., Doll, C., d'Entremont, R. P., Hu, B., Liang, S., Privette, J. L., and Roy, D.: First operational BRDF, albedo nadir reflectance products from MODIS, Remote Sensing of Environment, 83, 135-148, https://doi.org/10.1016/S0034-4257(02)00091-3, 2002.

Schaaf, C. B., Liu, J., Gao, F., and Strahler, A. H.: Aqua and Terra MODIS Albedo and Reflectance Anisotropy Products, in: Land Remote Sensing and Global Environmental Change: NASA's Earth Observing System and the Science of ASTER and MODIS, edited by: Ramachandran, B., Justice, C. O., and Abrams, M. J., Springer New York, New York, NY, 549-561, 2011.

Shi, G., Wang, H., Wang, B., Li, W., Gong, S., Zhao, T., and Aoki, T.: Sensitivity Experiments on the Effects of Optical Properties of Dust Aerosols on Their Radiative Forcing under Clear Sky Condition, Journal of The Meteorological Society of Japan - J METEOROL SOC JPN, 83A, 333-346, 10.2151/jmsj.83A.333, 2005.

Slingo, A., Ackerman, T. P., Allan, R. P., Kassianov, E. I., McFarlane, S. A., Robinson, G. J., Barnard, J. C., Miller, M. A., Harries, J. E., Russell, J. E., and Dewitte, S.: Observations of the impact of a major Saharan dust storm on the atmospheric radiation balance, Geophysical Research Letters, 33, 10.1029/2006gl027869, 2006.

Tanré, D., Kaufman, Y., Holben, B., Chatenet, B., Karnieli, A., Lavenu, F., Blarel, L., Dubovik, O., Remer, L., and Smirnov, A.: Climatology of dust aerosol size distribution and optical properties derived from remotely sensed data in the solar spectrum, Journal of Geophysical Research, 106, 10.1029/2000JD900663, 2001.

Tegen, I., Bierwirth, E., Heinold, B., Helmert, J., and Wendisch, M.: Effect of measured surface albedo on modeled Saharan dust solar radiative forcing, Journal of Geophysical Research: Atmospheres, 115, 10.1029/2009jd013764, 2010.

Textor, C., Schulz, M., Guibert, S., Kinne, S., Balkanski, Y., Bauer, S., Berntsen, T., Berglen, T., Boucher, O., Chin, M., Dentener, F., Diehl, T., Feichter, J., Fillmore, D., Ginoux, P., Gong, S., Grini, A., Hendricks, J., Horowitz, L., Huang, P., Isaksen, I. S. A., Iversen, T., Kloster, S., Koch, D., Kirkevåg, A., Kristjansson, J. E., Krol, M., Lauer, A., Lamarque, J. F., Liu, X., Montanaro, V., Myhre, G., Penner, J. E., Pitari, G., Reddy, M. S., Seland, Ø., Stier, P., Takemura, T., and Tie, X.: The effect of harmonized emissions on aerosol properties in global models – an AeroCom experiment, Atmos. Chem. Phys., 7, 4489-4501, 10.5194/acp-7-4489-2007, 2007.

Tian, L., Zhang, P., and Chen, L.: Estimation of the Dust Aerosol Shortwave Direct Forcing Over Land Based on an Equi-albedo Method From Satellite Measurements, Journal of Geophysical Research:

https://doi.org/10.5194/acp-2020-1113
Preprint. Discussion started: 14 January 2021

Atmospheric Chemistry and Physics
Open Access
EGU
Discussions

Atmospheres, 124, 8793-8807, 10.1029/2019JD030974, 2019.

Valenzuela, A., Olmo, F. J., Lyamani, H., Ant´®n, M., Quirantes, A., and Alados-Arboledas, L.: Aerosol radiative forcing during African desert dust events (2005¨C2010) over Southeastern Spain, Atmospheric Chemistry and Physics (ACP) & Discussions (ACPD), 2012.

Wang, Z., Zhang, H., Jing, X., and Wei, X.: Effect of non-spherical dust aerosol on its direct radiative forcing, Atmospheric Research, 120-121, 112-126, https://doi.org/10.1016/j.atmosres.2012.08.006, 2013.

Wielicki, B. A., Barkstrom, B. R., Baum, B. A., Charlock, T. P., Green, R. N., Kratz, D. P., Lee, R. B., Minnis, P., Smith, G. L., Takmeng, W., Young, D. F., Cess, R. D., Coakley, J. A., Crommelynck, D. A. H., Donner, L., Kandel, R., King, M. D., Miller, A. J., Ramanathan, V., Randall, D. A., Stowe, L. L., and Welch, R. M.: Clouds and the Earth's Radiant Energy System (CERES): algorithm overview, IEEE Transactions on Geoscience and Remote Sensing, 36, 1127-1141, 1998.

Xia, X., and Zong, X.: Shortwave versus longwave direct radiative forcing by Taklimakan dust aerosols, Geophysical Research Letters, 36, 10.1029/2009gl037237, 2009.

Zhang, J., Christopher, S. A., Remer, L. A., and Kaufman, Y. J.: Shortwave aerosol radiative forcing over cloud-free oceans from Terra: 2. Seasonal and global distributions, Journal of Geophysical Research (Atmospheres), 110, D10S24, 2005.

Zhang, P., Lu, N.-m., Hu, X.-q., and Dong, C.-h.: Identification and physical retrieval of dust storm using three MODIS thermal IR channels, Global and Planetary Change, 52, 197-206, https://doi.org/10.1016/j.gloplacha.2006.02.014, 2006.

Zhao, C., Chen, S., Leung, L. R., Qian, Y., Kok, J. F., Zaveri, R. A., and Huang, J.: Uncertainty in modeling dust mass balance and radiative forcing from size parameterization, Atmos. Chem. Phys., 13, 10733-10753, 10.5194/acp-13-10733-2013, 2013.